

Published in final edited form as:

DNA Repair (Amst). 2012 May 1; 11(5): 502–510. doi:10.1016/j.dnarep.2012.02.005.

Alkbh2 protects against lethality and mutation in primary mouse embryonic fibroblasts

Stephanie L. Nay¹, Dong-Hyun Lee^{2,†,‡}, Steven E. Bates^{1,‡}, and Timothy R. O'Connor¹

¹Biology Division, City of Hope National Medical Center, 1450 East Duarte Road, Duarte, CA 91010

²Beckman Research Institute, and Irell and Manella Graduate School of Biological Sciences, City of Hope National Medical Center, 1450 East Duarte Road, Duarte, CA 91010

Abstract

Alkylating agents modify DNA and RNA forming adducts that disrupt replication and transcription, trigger cell cycle checkpoints and/or initiate apoptosis. If left unrepaired, some of the damage can be cytotoxic and/or mutagenic. In *Escherichia coli*, the alkylation repair protein B (AlkB) provides one form of resistance to alkylating agents by eliminating mainly 1-methyladenine and 3-methylcytosine, thereby increasing survival and preventing mutation. To examine the biological role of the mammalian AlkB homologs Alkbh2 and Alkbh3, which both have similar enzymatic activities to that of AlkB, we evaluated the survival and mutagenesis of primary Big Blue mouse embryonic fibroblasts (MEFs) that had targeted deletions in the *Alkbh2* or *Alkbh3* genes. Both Alkbh2- and Alkbh3-deficient MEFs were ~2-fold more sensitive to methyl methanesulfonate (MMS) induced cytotoxicity compared to the wild type control cells. Spontaneous mutant frequencies were similar for the wild type, *Alkbh2*^{-/-} and *Alkbh3*^{-/-} MEFs (average- 1.3×10^{-5}). However, despite the similar survival of the two mutant MEFs after MMS treatment, only the Alkbh2-deficient MEFs showed a statistically significant increase in mutant frequency compared to wild type MEFs after MMS treatment. Therefore, although both Alkbh2 and Alkbh3 can protect against MMS-induced cell death, only Alkbh2 shows statistically significant protection of MEF DNA against mutations following treatment with this exogenous methylating agent.

Keywords

DNA repair; AlkB homologs; Fe(II)/ α -ketoglutarate-dependent dioxygenases; mutagenesis

© 2012 Elsevier B.V. All rights reserved.

^{*}Corresponding author. Telephone: 626-301-8220, Fax: 626-930-5366, toconnor@coh.org (T.R. O'Connor).

[†]Dept. of Radiation Oncology, Dana Farber Cancer Institute, Harvard Medical School, Jimmy Fund Bldg. Room 509, Boston, MA 02115.

[‡]Both authors contributed equally to this work.

Publisher's Disclaimer: This is a PDF file of an unedited manuscript that has been accepted for publication. As a service to our customers we are providing this early version of the manuscript. The manuscript will undergo copyediting, typesetting, and review of the resulting proof before it is published in its final citable form. Please note that during the production process errors may be discovered which could affect the content, and all legal disclaimers that apply to the journal pertain.

Conflict of interest Statement

The authors declare there are no conflicts of interest.

Appendix A. Supplemental Information

1. Introduction

Two major parameters are of concern when studying DNA damage and repair: **survival** and **mutation**. Alkylating agents form DNA and RNA adducts that can cause cytotoxic and/or mutagenic effects if the damage is not repaired [1]. Because alkylating agents are present environmentally and also generated within the cell via oxidative metabolism, exposure to them is unavoidable. Therefore, removal of alkyl/methyl group damage to DNA and RNA is critical to maintain proper cellular function, prevent cell death, avoid mutations, and preserve genomic integrity.

Discovered first in *Escherichia coli*, alkylation protein B (AlkB) belongs to a super-family of Fe(II)/ α -ketoglutarate-dependent dioxygenases, with roles in histone demethylation[2], proline hydroxylation[3] and in the case of AlkB, DNA and RNA dealkylation. Dealkylation catalyzed by AlkB and its homologs occurs via transformation of α -KG into succinate, formaldehyde release, and restoration of the undamaged base [4–9]. The reaction catalyzed by AlkB is direct, requiring no DNA polymerases or synthesis. The major methylated bases repaired by AlkB are 1-methyladenine (1-meA) and 3-methylcytosine (3-meC), but in addition, 3-methylthymine, 1-methylguanine, ethylated bases, and some etheno bases are also eliminated from DNA by AlkB [10–13]. Lesions that are repaired by AlkB interfere with DNA base pairing and block replication and transcription [14]. In *E. coli* AlkB mutants, alkyl adducts accumulate, causing increased sensitivity to alkylating agents, particularly the S_N2 type, and increased mutation frequency for site specific adducts [15].

In mice, as in humans, the AlkB super-family is composed of nine AlkB homologs (Alkbh1–8 and Fto). Human ALKBH5 is a HIF-1 α responsive gene [16], whereas ALKBH3 and 8 possess RNA and tRNA demethylase activity, respectively [17–20]. ALKBH1, 2 and 3 on the other hand, can remove methyl adducts from DNA [8, 17, 18, 21, 22]. Evaluation of Alkbh2 and 3 in mammals has shown that, similar to AlkB-deficient *E. coli*, immortalized Alkbh2-deficient mouse embryonic fibroblasts (MEFs) are more sensitive to methyl methanesulfonate (MMS) cytotoxicity in comparison to immortalized wild type (WT) MEFs. However, immortalized Alkbh3-deficient MEFs manifest approximately the same cytotoxicity to MMS as the WT immortalized MEFs [23]. Interestingly, some mammalian *AlkBh* genes, including *Alkbh2* and *3*, have been implicated in prostate, brain, lung, and bladder cancers and play a role in sensitivity to cisplatin therapeutics [24–28]. However, the exact roles of Alkbh2 and Alkbh3 in mammalian cell survival and mutagenesis have yet to be established.

Therefore, in order to determine the mutagenic consequences of unrepaired S_N2 alkylation adducts, we generated mice with targeted deletions in *Alkbh2* or *Alkbh3* and crossed them with Big Blue mice harboring λ LIZ reporter constructs. We then examined the survival of primary MEFs in response to MMS exposure and used the *cII* reporter to determine the spontaneous and MMS-induced mutant frequencies and mutation spectra for each MEF genotype.

2. Materials and Methods

2.1 Chemicals, proteins, molecular biology

Restriction enzymes were obtained from New England Biolabs (Ipswich, MA). All molecular biology methods, including cloning, and polymerase chain reaction (PCR) were performed using standard protocols [29].

2.2 *Alkbh2* and *Alkbh3* targeted deletions in mouse embryonic stem cells

Targeted disruption was performed in Y129 mouse embryonic stem cells (mESCs) to remove exons that contain critical active site residues in either the *Alkbh2* or *Alkbh3* gene [18]. Plasmid constructs with 5' and 3' arms were generated to eliminate either exon 4 (*Alkbh2*) or 7 (*Alkbh3*) (Fig. 1). The linearized constructs were electroporated, allowed to undergo homologous recombination, and were then positively selected for G418 (Geneticin) resistance. A negative selection to reduce false positives from non-homologous recombination was also employed using diphtheria toxin. Individual G418-resistant colonies in 24-well plates were lysed and screened using long PCR to identify putative clones that underwent the correct recombination. Gene disruption to produce heterozygous mESCs was confirmed using Southern blot and PCR analysis.

2.3 Southern blot analysis of *Alkbh2* and *Alkbh3*

Genomic DNA from *Alkbh2* targeted mESCs was digested using BclI restriction endonuclease to produce either 1833 and 1461 bp fragments for the targeted event or a 2163 bp WT DNA fragment. Similarly, genomic DNA from *Alkbh3* targeted mESCs was digested using ScaI and ClaI to produce either 1687 and 2653 bp fragments, for the targeted event, or a 3248 bp WT fragment (Fig. 1). Electrophoresis of digested DNA was carried out prior to alkaline transfer, under vacuum for 2 h, to a charged nylon membrane. Transferred DNA was fixed by UV radiation and the membrane incubated in blocking solution for 1 h. DNA γ -[³²P]-dCTP probes, generated by linear PCR, against either the 5' or 3' arms were hybridized to the membrane, washed three times at 50°C, and probe signals detected by phosphorimaging using a Typhoon Phosphorimager (GE Healthcare, Piscataway, NJ).

2.4 Embryonic stem cell transfer and mouse breeding

To produce chimeric animals, *Alkbh2* or *Alkbh3* heterozygous mESCs were microinjected into mouse embryos at the blastocyst stage and implanted in female mice by the City of Hope Transgenic Mouse Core. Offspring from the chimeric mice were genotyped to insure that there was germ line transfer of the *Alkbh2* or *Alkbh3* genotype. Homozygous *Alkbh2* or *Alkbh3* knock-out mice were obtained and verified by genotyping. WT, *Alkbh2*- and *Alkbh3* knock-out strains were bred with Big Blue B6 mice (Agilent Technologies, Santa Clara, CA) in the City of Hope Animal Resource Center to create knock-out *Alkbh* mouse models with ~40 contiguous copies of a chromosomally integrated λ LIZ bacteriophage. The λ LIZ harbors the *cII* reporter gene that allows the determination of spontaneous and induced mutant frequencies. Big Blue mice crossed with the homozygous *Alkbh2* or *Alkbh3* knock-out mice were genotyped to verify the presence or absence of *Alkbh2/Alkbh3*, and the λ LIZ phage mutation reporter.

2.5 Genotyping/PCR

Mouse tail tissue (1–2 mm) was dissolved overnight at 55°C in 200 μ l 1X PBND Buffer (50 mM KCl, 10 mM Tris-HCl pH 8.3, 2.5 mM MgCl₂, 0.1 mg/ml Gelatin, 0.45% v/v NP-40, 0.45% v/v Tween-20) containing 0.05 μ g/ μ l Proteinase K. Oligodeoxynucleotide (ODN) primers were obtained from Integrated DNA Technologies, Inc. (Coralville, Iowa) and were used as indicated in Table 1. PCR conditions used were as follows: For *cII*: 1 cycle (95°C 3 min, 95°C 30 s, 60°C 1 min, 72°C 1 min), 29 cycles (95°C 30 s, 60°C 1 min, 72°C 1 min), 72°C 10 min, 4°C hold. For mouse *Alkbh2/3*: 1 cycle (95°C 5 min, 95°C 45 s, 58°C 1 min, 72°C 1 min), 29 cycles (95°C 45 s, 58°C 1 min, 72°C 1 min), 72°C 10 min, 4°C hold. PCR products were separated on 2.0% agarose gels by electrophoresis (Tris-HCl, acetate, EDTA buffer), then stained with ethidium bromide and visualized with UV light.

2.6 Mouse embryonic fibroblast isolation

Embryos were harvested from mice at approximately day 11 post-coitus, washed three times with 1X phosphate buffered saline (PBS) and placed into individual 15 ml falcon tubes. 500 μ l of collagenase type 4 (~66 U/ml) was added to each embryo followed by incubation at 37°C until digested. Cells were transferred into multiple 100 mm tissue culture dishes (Corning, Corning, NY) containing Dulbecco's Modified Eagle Medium (DMEM) (Mediatech Inc., Manassas, VA), supplemented with 10% fetal bovine serum (FBS) (Omega Scientific, Tarzana, CA) and 1X L-glutamine, penicillin and streptomycin solution (Life Technologies, Carlsbad, CA). The MEF cells were cultured thereafter in a temperature controlled 37°C/5% CO₂ incubator until 80–90% confluent, at which point frozen ampoules were prepared (5% DMSO, 30% FBS, 65% DMEM) and stored in liquid nitrogen.

2.7 Cell culture

Single ampoules of WT, *Alkbh2*, or *Alkbh3* knock-out MEF cells were thawed and cultured in DMEM, supplemented with 10% FBS and 1X L-glutamine, penicillin and streptomycin solution in a temperature controlled 37°C/5% CO₂ incubator. Cells were passaged at approximately 80–90% confluence, using a 0.05% trypsin-EDTA solution, prepared by diluting 0.25% trypsin-EDTA solution (Life Technologies) with 1X PBS.

2.8 Confirmation of targeted exon deletions in mouse embryonic fibroblasts

Nuclear DNA was extracted from *Alkbh2* or *Alkbh3* knock-out MEF cells and evaluated for the absence of *AlkBh2* Exon 4 or *AlkBh3* Exon 7 (Fig. 1), as well as the presence of *Neo* by PCR. ODN primers used were as indicated in Table 1. PCR conditions used were as follows: (m2E4/m3E7/neo) 1 cycle (95°C 3 min, 95°C 30 s 60°C 1 min, 72°C 1 min) 29 cycles (95°C 30 s 60°C 1 min, 72°C 1 min), 72°C 5 min, 4°C hold. PCR products were separated on a 2.0% agarose gel by electrophoresis (TAE buffer), then stained with ethidium bromide, and visualized with UV light.

2.9 Western blot analysis of *Alkbh 2* and *3* protein production in mouse embryonic fibroblasts

Protein was extracted from WT and *Alkbh2* or *Alkbh3* knock-out MEFs and evaluated for expression of *Alkbh2* and *Alkbh3* proteins. MEF cells were washed with 1X PBS and lysed with ice-cold RIPA buffer (20 mM Tris-HCl (pH 7.5), 150 mM NaCl, 1% NP-40, 0.5% sodium deoxycholate, 1 mM EDTA, 0.1% SDS), supplemented with protease inhibitor cocktail (Roche, Indianapolis, IN), just before use. Lysates were incubated on ice for 10 min, vortexed gently for 30 s and centrifuged (10 min, 1000 \times g, 4°C). Supernatants were collected and protein concentrations determined using the Bradford assay [30]. WT and *Alkbh2* or *Alkbh3* knock-out protein samples (50 μ g) were combined with 5X SDS-PAGE loading buffer and dH₂O, heated (5 min, 95°C) and separated by electrophoresis on 4 – 15% Mini Protean TGX SDS-PAGE gels (Bio-Rad Laboratories, Hercules, CA) (250 V, 25 min). Samples were transferred to 0.2 μ m PVDF membranes (Bio-Rad) (100 V, 1 h) using wet electro-transfer (0.2 M glycine, 25 mM Tris and 20% methanol). Membranes were blocked in Li-Cor Biosciences (Lincoln, Nebraska) Odyssey Infrared Imaging System Blocking Buffer (1 h, RT or overnight, 4°C), followed by incubation with anti-actin and anti-*Alkbh2* or -*Alkbh3* primary antibodies (Santa Cruz Biotechnology Inc., Bath, UK) (1:5000 in 50% (v/v) Odyssey Blocking Buffer/1X TBS) (1 h, RT or overnight, 4°C). Membranes were washed (3 \times 5 min) in 1X TBS-Tween (1/1000 (v/v)), incubated with anti-mouse IR800 and anti-rabbit IR700 secondary antibodies (Li-Cor Biosciences) (1:20,000 in 50% (v/v) Odyssey Blocking Buffer/1X TBS) (1 h, RT) and washed again (1X TBS-T, 3 \times 5 min). Detection of proteins was conducted using the Li-Cor Odyssey near-infrared Imaging Station.

2.10 Methyl methanesulfonate treatments for cell survival and mutation assays

MEFs were seeded in 6-well culture dishes at 1×10^6 cells/well. The following day MEFs were washed twice with 1X PBS and treated for 20 min with MMS (0 – 100 mM) in serum-free DMEM or with serum-free DMEM minus MMS. Following treatment, cells were washed twice with 1X PBS and fresh DMEM (10% FBS) media added. Sensitivity of each cell line to the S_N2 alkylating agent MMS was determined by Trypan Blue uptake in MEFs at 48 h post-MMS treatment. The lowest determined IC_{50} value, 4 mM, was utilized thereafter as the MMS treatment dose for *cII* mutation assays. WT and *Alkbh* knock-out MEFs were incubated in serum-free media with (12×150 mm) or without (3×150 mm) MMS, as described above. Following treatment, cells were incubated at 37°C/5% CO₂ for 5 days. Medium was replaced after 48 h and cells were passaged as necessary.

2.11 Genomic DNA isolation

Cells were trypsinized (0.05% trypsin), pooled from 4×150 mm culture dishes, pelleted, and washed twice with 1X PBS. Pellets were lysed, on ice for 5 min, with 5 ml Buffer A (0.3 M Sucrose, 60 mM KCl, 15 mM NaCl, 60 mM Tris-HCl, pH 8, 0.5 mM spermidine, 0.15 mM spermine, 2 mM EDTA) with 0.5% NP-40. Pelleted nuclei were obtained by centrifugation (5 min, 1000×g, 4°C). Buffer A with 0.5% NP-40 was decanted and replaced with 5 ml Buffer A. Pelleted nuclei were again centrifuged and Buffer A decanted prior to resuspension in equal volumes (2.5 ml) of Buffer B (150 mM NaCl, 5 mM EDTA pH 7.8), and Buffer C [20 mM Tris-HCl pH 8, 20 mM NaCl, 20 mM EDTA, 1% SDS, 600 µg/ml Proteinase K (added just before use)]. Samples were incubated at 37°C for 3 h then residual RNA was removed by the addition of RNase A (10 mg/ml) to a final concentration of 100 µg/ml, and incubation at 37°C for 1 h. DNA was extracted following standard phenol/chloroform protocols [31]. DNA in the aqueous phase was precipitated by addition of three volumes of cold 100% ethanol, incubation on ice for 30 min and centrifugation (15 min, 1000×g, 4°C). Precipitated genomic DNA was washed with 70% ethanol, centrifuged (15 min, 1000×g, 4°C), air-dried and re-suspended in 0.1X Tris-EDTA. Concentrations were determined using a NanoDrop spectrophotometer (Thermo Scientific, Wilmington, DE).

2.12 *cII* mutation assay

cII mutant frequency assays were carried out as indicated by the manufacturer (Agilent Technologies). Nuclear genomic DNA was extracted, as described above, then packaged into λ phage and infected into G1250 host *E. coli* cells. Infected host cells were plated at different dilutions and cultured at a non-selective temperature (37°C) to determine the total number of phage screened. Undiluted host cells were also cultured at the selective temperature (24°C) for lysogenic or lytic growth. Mutant frequencies were determined for WT, *Alkbh2*, and *Alkbh3* knock-out MEFs obtained from single embryos, and were repeated for two separate litters. In each case over 3×10^5 phage plaques were screened for mutations.

2.13 Mutant sequence analysis

Mutant *cII* sequences were amplified by PCR, as recommended by the manufacturer (Agilent Technologies, Santa Clara CA), and sequenced by Laragen, Inc. (Culver City, CA) or the City of Hope Sequencing Core (Duarte, CA). Sequence alignments were prepared with ClustalW2 sequence analysis software.

2.14 Statistical analysis

Following recommendations for mutation spectra [32, 33], significance probabilities for aggregated data were calculated from chi-square statistics referred to Monte Carlo null distributions, using StatXact 7.0.0 (Cytel Software Corporation, Cambridge, MA). A global

test of Table 2 was used to support experiment-wide significance. Tests of Poisson rates were used for comparisons of single mutation types. Significance of hotspots was established by reference to a Monte Carlo simulation of a Poisson process, using R version 2.14.0.

3. Results

3.1 Generation of mice with targeted deletions in *Alkbh2* or *Alkbh3*

All AlkB homologs share a conserved active site that contains three critical domains; the nucleotide recognition lid, the N-terminal extension and the catalytic core [34–36]. In the mouse AlkB homologs *Alkbh2* and *Alkbh3*, these domains span exons 2–4 and 2–9, respectively. Therefore, targeted deletion of exon 4 in *Alkbh2* or exon 7 in *Alkbh3* was carried out via homologous recombination in mESCs and confirmed by Southern blot analysis (Fig. 1). Following the transfer of heterozygous mESCs into blastocysts, chimeric offspring were isolated and used to establish colonies of *Alkbh2*- or *Alkbh3*-deficient mice. WT and *Alkbh2*- or *Alkbh3*-deficient mice were then bred with Big Blue λ LIZ mutation reporter mice to establish WT, *Alkbh2*- and *Alkbh3*-deficient mouse colonies that contained the mutation reporter construct. Breeding of Big Blue *Alkbh2*- and *Alkbh3*-deficient mouse colonies with one another was also conducted to obtain *Alkbh2/3* double knock-out mouse colonies. These colonies were used to generate the MEF cells used in this study. As reported previously, no obvious pathologies, including changes in fertility or longevity were observed [23].

3.2 Isolation of primary wild-type, *Alkbh2*^{-/-}, or *Alkbh3*^{-/-} mouse embryonic fibroblasts

Because spontaneous cellular immortalization of MEFs generally results in a large number of changes to the genome and can alter genomic stability, we used primary MEF cells in these experiments. Primary MEF cells were isolated from individual embryos harvested at ~11 day post-coitus and were screened for the targeted *Alkbh2* or *Alkbh3* deletions using PCR analysis (Fig. 2). Western blot analysis of WT and *Alkbh2*- or *Alkbh3*-deficient MEF protein extracts revealed that MEFs with targeted deletions in *Alkbh2* or *Alkbh3* do not express the respective proteins (Supplemental Fig. 1). For each experiment, two separate, non-litter mate embryos were used to ensure that the results obtained were not litter-dependent. MEFs used in this study were passage seven or less. Though *Alkbh2/3* double knock-out mice are viable, on multiple occasions, and in the hands of different individuals, MEFs prepared from various embryos were not able to be cultured beyond passage three. As experiments were conducted using MEFs prepared from single embryos, the number of cells required for viability, activity, and *cII* mutation assays precluded use of the primary *Alkbh2/3* double knock-out MEFs.

3.3 Both *Alkbh2*^{-/-} and *Alkbh3*^{-/-} primary mouse embryonic fibroblasts are more sensitive than wild-type cells to methyl methanesulfonate

Exposure to MMS induces a variety of DNA adducts, including 1-meA and 3-meC, both of which halt replication and can result in lethality at high MMS doses. To assess the protective roles of *Alkbh2* and *Alkbh3* against chemically-induced cytotoxicity, WT, *Alkbh2*^{-/-} and *Alkbh3*^{-/-} primary MEFs were treated with MMS and then assayed for cytotoxicity based on membrane integrity (Fig. 3a). Both the *Alkbh2*- and *Alkbh3*-deficient lines showed an almost 2-fold, statistically significant lower IC₅₀ value compared with WT primary MEFs (Fig. 3b).

3.4 Alkbh2 has a greater protective effect against chromosomal mutations than Alkbh3

In the absence of Alkbh2 or Alkbh3, cell viability of primary MEFs is significantly reduced in response to MMS treatment. Since a deficiency of Alkbh2 or Alkbh3 could result in adduct persistence and thereby increase the mutant frequency, we compared spontaneous and MMS-induced mutant frequencies in primary WT, *Alkbh2*^{-/-}, and *Alkbh3*^{-/-} MEFs. The three primary MEF lines were treated with and without 4 mM MMS in serum-free medium and then allowed to replicate over a five day period. Genomic DNA from the MEFs was isolated and used in a phage packaging reaction to infect G1250 host cells, which allowed the detection of mutations in the *cII* gene of the λ LIZ reporter (Supplemental Fig. 2). The 1.5- and 2.7-fold increase in mutant frequency observed in untreated *Alkbh2*^{-/-} and *Alkbh3*^{-/-} MEFs did not show a statistically significant difference from that of WT MEFs. However, following MMS treatment, the mutant frequency for *Alkbh2*^{-/-} MEFs was significantly increased compared to treated WT (~7-fold) and the spontaneous *Alkbh2*^{-/-} MEF mutant frequency (~6-fold). In contrast to the *Alkbh2*^{-/-} MEFs, the increase in mutant frequency in MMS treated *Alkbh3*^{-/-} MEFs (~3-fold) was not statistically significant, compared to the WT control. Comparison of the induced mutant frequency (observed – spontaneous) in WT and Alkbh2- or Alkbh3-deficient MEFs showed increases of 4.0, 70.5, and 12.2 ($\times 10^{-6}$), respectively (Fig. 4). Similarly, *Alkbh3*^{-/-} MEFs exhibited ~3-fold difference compared to WT MEFs, which again was not significant. *Alkbh2*^{-/-} MEFs, on the other hand, exhibited a statistically significant 17.6-fold increase in induced mutant frequency, compared to WT MEFs. Therefore, the decreased survival of *Alkbh2*^{-/-} MEFs following MMS treatment was accompanied by a significant increase in mutant frequency. However, although *Alkbh3*^{-/-} cells also showed decreased survival in response to MMS treatment, there was no corresponding statistically significant increase in MMS-induced mutants. Therefore, although both *Alkbh2*^{-/-} and *Alkbh3*^{-/-} primary MEFs provide equal protection against MMS treatment with similar substrate specificities and protect against similar types of mutations, Alkbh2 has a greater protective effect against mutations than Alkbh3.

3.5 Spontaneous C→A transversion and C→T transition mutations are increased in Alkbh2^{-/-} mouse embryonic fibroblasts

To examine the type of mutations induced, the *cII* gene in the λ LIZ reporter from at least 29 mutant phage plaques with spontaneous mutations, from each primary MEF line, were sequenced (Table 2, Supplemental Figure 3). Compared to WT cells, *Alkbh2*^{-/-} MEFs showed a different spontaneous mutation spectrum (p=0.006). The most striking feature was the large increase in C→A mutations (2.7-fold, p=0.0001). There was also a smaller but noticeable increase in the number of C→T mutations (1.6-fold, p=0.06).

3.6 Spontaneous C→T transition and C→A transversion mutations are increased in Alkbh3^{-/-} mouse embryonic fibroblasts

The major change in the mutation spectrum of *Alkbh3*^{-/-} MEFs compared to WT is the increase in C→T mutations (2.6-fold, p=0.003). The number of C→A mutations was also increased (1.6-fold, p=0.05), but the statistical significance was less than that observed for the *Alkbh2*^{-/-} MEF spontaneous mutations. The increase in C→T (G→A on the complementary strand) mutations in both mutants was unexpected, because that class of transition mutation is generally associated with O6-methylguanine adduct repair.

3.7 Methyl methanesulfonate-induced C→A transversions and C→T transitions predominate in the Alkbh2^{-/-} mutation spectrum

Although MMS treatment significantly increased the mutant frequency in *Alkbh2*^{-/-} MEFs, the most prevalent type of mutation in *Alkbh2*^{-/-} MEFs remained C→A transversions (3.0-

fold). There were also increased C→T mutations. Therefore, although the mutation frequency increased upon MMS treatment, the types of mutations induced were similar to the spontaneous mutations. However, there was an observed, but non-significant increase in A→T transitions in MMS treated *Alkbh2*^{-/-} MEFs compared to the low frequency of A→T transitions found in the spontaneous *Alkbh2*^{-/-} MEF mutations (p=0.14). Another difference between WT and *Alkbh2*^{-/-} following MMS treatment is the absence of any deletion mutations in the *Alkbh2*^{-/-} mutation spectrum. Therefore, the C→A and C→T increases are noteworthy in both the spontaneous and MMS-induced *Alkbh2*^{-/-} MEFs, compared to the WT MEFs, whereas the A→T transitions increased only upon MMS exposure.

3.8 Methyl methanesulfonate-induced C→T transitions and C→A transversions represent the major changes in the *Alkbh3*^{-/-} mutation spectrum

The MMS treatment of *Alkbh3*^{-/-} MEFs primarily increased G→T (1.4-fold) mutations compared to the MMS treated WT MEFs. C→T mutations were also increased compared to WT. Again there was an increase in the number of A→T mutations observed for the *Alkbh3*^{-/-} following MMS treatment.

3.9 Mutation hot spots in *Alkbh2*^{-/-} MEFs are associated with C→A transversions

Monte Carlo simulation of 1000 samples from a homogeneous Poisson process suggests six mutations at a given position as a threshold for statistical significance. Given that criterion, only two positions appeared as hot spots and both of these occurred in DNA from *Alkbh2*^{-/-} MEF cells. In untreated *Alkbh2*^{-/-} MEF cells, a hot spot with 17 G→T (C→A) spontaneous mutations was observed at position 159 (Fig. 6). In the MMS treated *Alkbh2*^{-/-} MEFs, the mutation analysis, revealed a single hot spot with eight G→T (C→A) mutations at position 301 (Fig. 6). No other hot spots for mutations were detected in any of the other primary MEFs using this analysis (Fig. 5 and 7). This result appears to be consistent with the observation that MMS treated primary *Alkbh2*^{-/-} MEFs have a significantly higher mutant frequency than that observed for MMS treated WT or *Alkbh3*^{-/-} MEFs.

4. Discussion

Exposure to alkylating agents, originating from both the environment and within the cell, means that subsequent generation of alkyl and methyl adducts in DNA and RNA, is virtually unavoidable. Consequently, the removal of alkyl/methyl groups from DNA and RNA is critical for cellular function, because unrepaired adducts have cytotoxic and/or mutagenic effects. At present, identification and definition of the specific biological roles of mammalian proteins involved in repair of DNA alkylation adducts is an ongoing process. In *E. coli*, AlkB repairs alkylation damage and protects cells during their adaptive response to alkylating agents [7, 37]. However, humans possess nine *E. coli* AlkB homologs (ALKBH1–8 and FTO), the biological roles of which are not well understood. Fortunately, conservation of mammalian AlkB homologs in mice and humans provides an important laboratory model for the study of these repair proteins in mammalian systems. Previous studies have shown not only conservation of the active site, but also comparable activities between mouse and human AlkB homologs [18].

Currently, three ALKBH proteins, ALKBH1–3, are known to remove 1-meA and 3-meC adducts from DNA that would otherwise disrupt replication and transcription, triggering cell cycle checkpoints and apoptosis [17, 21, 22, 36, 38, 39]. ALKBH1 is a mitochondrial protein [22], so we have concentrated on elucidating the roles of ALKBH2 and ALKBH3 that are considered to be nuclear proteins [40]. Despite what is known about the repair activities of these proteins, their actual biological roles have yet to be established. Generation of mouse models with targeted deletions in *Alkbh2* or *Alkbh3*, and integration

with the λ LIZ transgene system, has allowed us not only to determine the spontaneous and MMS-induced mutant frequencies in primary MEFs deficient in either of these two homologs, but also to generate mutation spectra and maps specific for each deficient cell line.

Our results, using primary MEFs, support previous findings using an immortalized Alkbh2-deficient cell line, in that the absence of Alkbh2 causes increased susceptibility to S_N2 alkylating agents, specifically MMS [23]. However in contrast to that original report, we note that in addition to Alkbh2-deficient primary MEFs, Alkbh3-deficient MEFs are also at least twice as sensitive to MMS compared to wild type MEFs. That suggests that there is a difference between the survival of primary and immortalized Alkbh3-deficient cells.

In spite of the difference in survival noted for Alkbh3-deficient primary fibroblasts, a significant effect on the mutant frequency was observed only for Alkbh2-deficient primary MEFs. However, as shown in a recent study, various human cell types depend differently on ALKBH2 and 3. Therefore, it is possible that in transformed cells, generated from various Alkbh3-deficient mouse tissue types, the effect on the mutant frequency could be significant [24]. Moreover, it is still uncertain which adducts are responsible for the increased sensitivity to MMS observed in the MEFs and any mutagenic consequences to the cell in the absence of repair.

Until this study, the mutagenic potential of 1-meA and 3-meC DNA adducts had only been determined in AlkB-deficient *E. coli* cells [15]. In that report, 3-meC adducts introduced into plasmids were mutagenic, with 90% of the mutations being associated with C→A and C→G transversions and C→T transitions. In contrast, 1-meA adducts were not significantly mutagenic and exhibited a mutation frequency of only ~5%, which resulted in A→T transition mutations [15]. Therefore, to provide a better understanding of the biological role of mammalian AlkB homologs, we studied the mutagenic impact of Alkbh2 or Alkbh3 homolog deletion by examining spontaneous and MMS-induced mutations in the *cII* transgene from primary Big Blue WT, *Alkbh2*^{-/-} and *Alkbh3*^{-/-} MEF cells.

Similar to mutations produced by the unique 3-meC adducts in AlkB-deficient *E. coli* [15], *Alkbh2*^{-/-} and *Alkbh3*^{-/-} MEFs show increased spontaneous C→A mutations (50% and 30%, respectively) compared to WT (17%) and increased spontaneous C→T transversions (20% and 34%, respectively) compared to WT (10%). These results suggest that the repair of 3-meC adducts in ssDNA and dsDNA is critical for the maintenance of genomic integrity and that Alkbh2 and Alkbh3 are the primary repair proteins for these adducts. Interestingly, following MMS treatment, Alkbh2- and Alkbh3-deficient MEFs not only show increases in C→A mutations (34% and 21%, respectively) and C→T transversions (32% and 28%, respectively) compared to WT (C→A, 19% and C→T 22%), they also exhibit increases in the frequency of A→T mutations (18% and 26%, respectively), comparable to those observed in the WT MEFs (11%). In *E. coli*, 1-meA adducts are essentially non-mutagenic (~5% T→A) [15]. However these adducts are generated almost 2-fold more in ssDNA and 4-fold more in dsDNA than 3-meC [41] and also accumulate in Alkbh2-deficient immortalized MEFs [23].

1-meG and 3-meT are formed at low frequencies (< 0.5%) in ssDNA, both *in vitro* and *in vivo*, by S_N2 methylating agents [41]. The evaluation of mutation frequencies in *E. coli* using a restriction endonuclease and post-labeling analysis of mutation (REAP) assay indicated that unrepaired 1-meG and 3-meT DNA adducts are mutagenic (20% G→A, 50% G→T and 40% T→A, 10% T→C, respectively) [15]. Mammalian Alkbh2 and Alkbh3 also repair 1-meG and 3-meT adducts [11, 13], which could contribute to the increased mutant frequencies observed in the Alkbh2- and Alkbh3-deficient MEFs after MMS treatment.

However, because the frequency of 1-meG or 3-meT formation by MMS is much less than that of 1-meA and 3-meC, the probability of observing mutations due to those adducts is low [41]. Therefore, the best way to determine which adducts are responsible for each type of mutation will require the use of single adduct lesions in episomes that replicate in mouse cells followed by analysis of the mutations produced. [42].

Thus, determining the frequency of each adduct that occurs spontaneously and in response to MMS treatment, using the Alkbh-deficient mouse models, will greatly contribute to our understanding of the rate of occurrence and mutagenic potential of this type of DNA damage. Furthermore, determining the repair capacity of the Alkbh2 and Alkbh3 proteins for each adduct will be critical for identifying the biological role, in the cell, of this family of proteins. In addition, this information, combined with studies of the mouse models, will further our understanding of the role played by Alkbh2 and Alkbh3 in certain cancers and may provide insight that can be used for predictive diagnosis or potential therapeutics.

Supplementary Material

Refer to Web version on PubMed Central for supplementary material.

Acknowledgments

We thank the City of Hope, Payson Foundation, TRDRP, and City of Hope Cancer Center for funding and Drs. Walter Tsark, Seung-Gi Jin, and Margaret Morgan for their scientific expertise and help with manuscript preparation. Dr. Jeffrey Longmate is gratefully acknowledged for his assistance with the statistical analysis of the mutation spectra and maps.

Abbreviations

MMS	methylmethane sulfonate
ds	double-stranded
ss	single-stranded
ODN	oligodeoxynucleotides
α-KGFdiO	α -ketoglutarate Fe(II) dioxygenase
MEFs	mouse embryonic fibroblasts
mESCs	mouse embryonic stem cells. All gene names are in italics with human gene names all capitalized and mouse gene names with only the first letter capitalized, and <i>E. coli</i> gene names all lower case. Gene product (protein) names are non-italicized with the same convention as gene names for human and mouse. For <i>E. coli</i> , protein names have only the first letter capitalized

References

1. Drablos F, Feyzi E, Aas PA, Vaagbo CB, Kavli B, Bratlie MS, Pena-Diaz J, Otterlei M, Slupphaug G, Krokan HE. Alkylation damage in DNA and RNA--repair mechanisms and medical significance. *DNA Repair (Amst)*. 2004; 3:1389–1407. [PubMed: 15380096]
2. Shin S, Janknecht R. Diversity within the JMJD2 histone demethylase family. *Biochem Biophys Res Commun*. 2007; 353:973–977. [PubMed: 17207460]
3. Flashman E, Davies SL, Yeoh KK, Schofield CJ. Investigating the dependence of the hypoxia-inducible factor hydroxylases (factor inhibiting HIF and prolyl hydroxylase domain 2) on ascorbate and other reducing agents. *Biochem J*. 2010; 427:135–142. [PubMed: 20055761]

4. Begley TJ, Samson LD. AlkB mystery solved: oxidative demethylation of N1-methyladenine and N3-methylcytosine adducts by a direct reversal mechanism. *Trends Biochem Sci.* 2003; 28:2–5. [PubMed: 12517444]
5. Bleijlevens B, Shivarattan T, Flashman E, Yang Y, Simpson PJ, Koivisto P, Sedgwick B, Schofield CJ, Matthews SJ. Dynamic states of the DNA repair enzyme AlkB regulate product release. *EMBO Rep.* 2008; 9:872–877. [PubMed: 18617893]
6. Falnes PO, Johansen RF, Seeberg E. AlkB-mediated oxidative demethylation reverses DNA damage in *Escherichia coli*. *Nature.* 2002; 419:178–182. [PubMed: 12226668]
7. Kataoka H, Sekiguchi M. Molecular cloning and characterization of the alkB gene of *Escherichia coli*. *Mol Gen Genet.* 1985; 198:263–269. [PubMed: 3884973]
8. Mishina Y, He C. Oxidative dealkylation DNA repair mediated by the mononuclear nonheme iron AlkB proteins. *J Inorg Biochem.* 2006; 100:670–678. [PubMed: 16469386]
9. Trewick SC, Henshaw TF, Hausinger RP, Lindahl T, Sedgwick B. Oxidative demethylation by *Escherichia coli* AlkB directly reverts DNA base damage. *Nature.* 2002; 419:174–178. [PubMed: 12226667]
10. Delaney JC, Smeester L, Wong C, Frick LE, Taghizadeh K, Wishnok JS, Drennan CL, Samson LD, Essigmann JM. AlkB reverses etheno DNA lesions caused by lipid oxidation in vitro and in vivo. *Nat Struct Mol Biol.* 2005; 12:855–860. [PubMed: 16200073]
11. Falnes PO. Repair of 3-methylthymine and 1-methylguanine lesions by bacterial and human AlkB proteins. *Nucleic Acids Res.* 2004; 32:6260–6267. [PubMed: 15576352]
12. Frick LE, Delaney JC, Wong C, Drennan CL, Essigmann JM. Alleviation of 1,N6-ethanoadenine genotoxicity by the *Escherichia coli* adaptive response protein AlkB. *Proc Natl Acad Sci U S A.* 2007; 104:755–760. [PubMed: 17213319]
13. Koivisto P, Robins P, Lindahl T, Sedgwick B. Demethylation of 3-methylthymine in DNA by bacterial and human DNA dioxygenases. *J Biol Chem.* 2004; 279:40470–40474. [PubMed: 15269201]
14. Groth P, Auslander S, Majumder MM, Schultz N, Johansson F, Petermann E, Helleday T. Methylated DNA causes a physical block to replication forks independently of damage signaling, O(6)-methylguanine or DNA single-strand breaks and results in DNA damage. *J Mol Biol.* 2007; 402:70–82. [PubMed: 20643142]
15. Delaney JC, Essigmann JM. Mutagenesis, genotoxicity, and repair of 1-methyladenine, 3-alkylcytosines, 1-methylguanine, and 3-methylthymine in alkB *Escherichia coli*. *Proc Natl Acad Sci U S A.* 2004; 101:14051–14056. [PubMed: 15381779]
16. Thalhammer A, Bencokova Z, Poole R, Loenarz C, Adam L, O'Flaherty L, Schödel J, Mole D, Giaslaktiotis K, Schofield CJ, Hammond EM, Ratcliffe PJ, Pollard PJ. Human AlkB homologue 5 is a nuclear 2-oxoglutarate dependent oxygenase and a direct target of hypoxia-inducible factor 1 α (HIF-1 α). *PLoS One.* 2011; 6
17. Aas PA, Otterlei M, Falnes PO, Vagbo CB, Skorpen F, Akbari M, Sundheim O, Bjoras M, Slupphaug G, Seeberg E, Krokan HE. Human and bacterial oxidative demethylases repair alkylation damage in both RNA and DNA. *Nature.* 2003; 421:859–863. [PubMed: 12594517]
18. Lee DH, Jin SG, Cai S, Chen Y, Pfeifer GP, O'Connor TR. Repair of methylation damage in DNA and RNA by mammalian AlkB homologues. *J Biol Chem.* 2005; 280:39448–39459. [PubMed: 16174769]
19. Songe-Moller L, van den Born E, Leihne V, Vagbo CB, Kristoffersen T, Krokan HE, Kirpekar F, Falnes PO, Klungland A. Mammalian ALKBH8 possesses tRNA methyltransferase activity required for the biogenesis of multiple wobble uridine modifications implicated in translational decoding. *Mol Cell Biol.* 2010; 30:1814–1827. [PubMed: 20123966]
20. Fu D, Brophy J, Chan C, KA A, U B, RS P, PC D, TJ B, LD S. Human AlkB homolog ABH8 is a tRNA methyltransferase required for wobble uridine modification and DNA damage survival. *Mol Cell Biol.* 2010:2449–2459. [PubMed: 20308323]
21. Duncan T, Trewick SC, Koivisto P, Bates PA, Lindahl T, Sedgwick B. Reversal of DNA alkylation damage by two human dioxygenases. *Proc Natl Acad Sci U S A.* 2002; 99:16660–16665. [PubMed: 12486230]

22. Westbye MP, Feyzi E, Aas PA, Vagbo CB, Talstad VA, Kavli B, Hagen L, Sundheim O, Akbari M, Liabakk NB, Slupphaug G, Otterlei M, Krokan HE. Human AlkB homolog 1 is a mitochondrial protein that demethylates 3-methylcytosine in DNA and RNA. *J Biol Chem.* 2008; 283:25046–25056. [PubMed: 18603530]
23. Ringvoll J, Nordstrand LM, Vagbo CB, Talstad V, Reite K, Aas PA, Lauritzen KH, Liabakk NB, Bjork A, Doughty RW, Falnes PO, Krokan HE, Klungland A. Repair deficient mice reveal mABH2 as the primary oxidative demethylase for repairing 1meA and 3meC lesions in DNA. *EMBO J.* 2006; 25:2189–2198. [PubMed: 16642038]
24. Dango S, Mosammaparast N, Sowa M, Xiong L, Wu F, Park K, Rubin M, Gygi S, Harper J, Shi Y. DNA Unwinding by ASCC3 Helicase Is Coupled to ALKBH3-Dependent DNA Alkylation Repair and Cancer Cell Proliferation. *Molecular Cell.* 2011:373–384. [PubMed: 22055184]
25. Konishi N, Nakamura M, Ishida E, Shimada K, Mitsui E, Yoshikawa R, Yamamoto H, Tsujikawa K. High expression of a new marker PCA-1 in human prostate carcinoma. *Clin Cancer Res.* 2005; 11:5090–5097. [PubMed: 16033822]
26. Shimada K, Nakamura M, Anai S, De Velasco M, Tanaka M, Tsujikawa K, Ouji Y, Konishi N. A novel human AlkB homologue, ALKBH8, contributes to human bladder cancer progression. *Cancer Res.* 2009; 69:3157–3164. [PubMed: 19293182]
27. Tasaki M, Shimada K, Kimura H, Tsujikawa K, Konishi N. ALKBH3, a human AlkB homologue, contributes to cell survival in human non-small-cell lung cancer. *British Journal of Cancer.* 2011:1–7.
28. Wu SS, Xu W, Liu S, Chen B, Wang XL, Wang Y, Liu SF, Wu JQ. Downregulation of ALKBH2 increases cisplatin sensitivity in H1299 lung cancer cells. *Acta Pharmacologica Sinica.* 2011:1–6. [PubMed: 21170081]
29. Ausubel, FM.; Brent, R.; Kingston, RE.; Moore, DD.; Seidman, JG.; Smith, JA.; Struhl, K. *Current Protocols in Molecular Biology.* In: Ausubel, FM., editor. Greene Publishing Associates. New York: 1994. p. 5,300
30. Bradford MM. A rapid and sensitive method for the quantitation of microgram quantities of protein utilizing the principle of protein-dye binding. *Analytical Biochemistry.* 1976; 72:248–254. [PubMed: 942051]
31. Ye, N. Heterogenous Repair of N-Methylpurines at the Nucleotide Level in Normal Human Cells. In: Holmquist, GP.; O'Connor, TR., editors. *J. Mol. Biol.* Vol. 284. 1998. p. 269-285.
32. Adams TW, Skopek TR. Statistical Test for the Comparison of Samples from Mutational Spectra. *J. Mol. Biol.* 1987; 194:391–396. [PubMed: 3305960]
33. Piegorsch WW, Bailer JA. Statistical Approaches for Analyzing Mutational Spectra: Some Recommendations for Categorical Data. *Genetics.* 1994; 136:403–416. [PubMed: 8138174]
34. Kurowski MA, Bhagwat AS, Papaj G, Bujnicki JM. Phylogenomic identification of five new human homologs of the DNA repair enzyme AlkB. *BMC Genomics.* 2003; 4:48. [PubMed: 14667252]
35. Sundheim O, Vagbo CB, Bjaras M, Sousa MM, Talstad V, Aas PA, Drablos F, Krokan HE, Tainer JA, Slupphaug G. Human ABH3 structure and key residues for oxidative demethylation to reverse DNA/RNA damage. *EMBO J.* 2006; 25:3389–3397. [PubMed: 16858410]
36. Wei YF, Carter KC, Wang RP, Shell BK. Molecular cloning and functional analysis of a human cDNA encoding an Escherichia coli AlkB homolog, a protein involved in DNA alkylation damage repair. *Nucleic Acids Res.* 1996; 24:931–937. [PubMed: 8600462]
37. Kataoka H, Yamamoto Y, Sekiguchi M. A new gene (alkB) of Escherichia coli that controls sensitivity to methyl methane sulfonate. *J Bacteriol.* 1983; 153:1301–1307. [PubMed: 6337994]
38. Falnes PO, Bjaras M, Aas PA, Sundheim O, Seeberg E. Substrate specificities of bacterial and human AlkB proteins. *Nucleic Acids Res.* 2004; 32:3456–3461. [PubMed: 15229293]
39. Sedgwick B, Robins P, Lindahl T. Direct removal of alkylation damage from DNA by AlkB and related DNA dioxygenases. *Methods Enzymol.* 2006; 408:108–120. [PubMed: 16793366]
40. Tsujikawa K, Koike K, Kitae K, Shinkawa A, Arima H, Suzuki T, Tsuchiya M, Makino Y, Furukawa T, Konishi N, Yamamoto H. Expression and sub-cellular localization of human ABH family molecules. *J Cell Mol Med.* 11:1105–1116. [PubMed: 17979886]

41. Singer, B.; Grunberger, D. *Molecular Biology of Mutagens and Carcinogens*. 1 ed.. New York: Plenum; 1983. p. 347
42. Yuan B, You C, Andersen N, Jiang Y, Moriya M, O'Connor T, Wang Y. The Roles of DNA Polymerases κ and ι in the Error-free Bypass of N2-carboxyalkyl-dG Lesions in Mammalian Cells. *J Biol Chem*. 2011;1–16.

Highlights

- Alkbh2 and Alkbh3 are Fe(II)/ α -ketoglutarate-dependent dioxygenases both protect primary MEFs from cytotoxic alkylation damage.
- Only Alkbh2 protects primary cells from mutagenic alkylation damage.
- Alkbh2 and Alkbh3 have similar substrate specificity but provide different protection against alkylation damage.
- Alkbh2 and Alkbh3 protection against spontaneous and induced C→T and C→A mutations and methylmethane sulfonate induced A→T mutations.

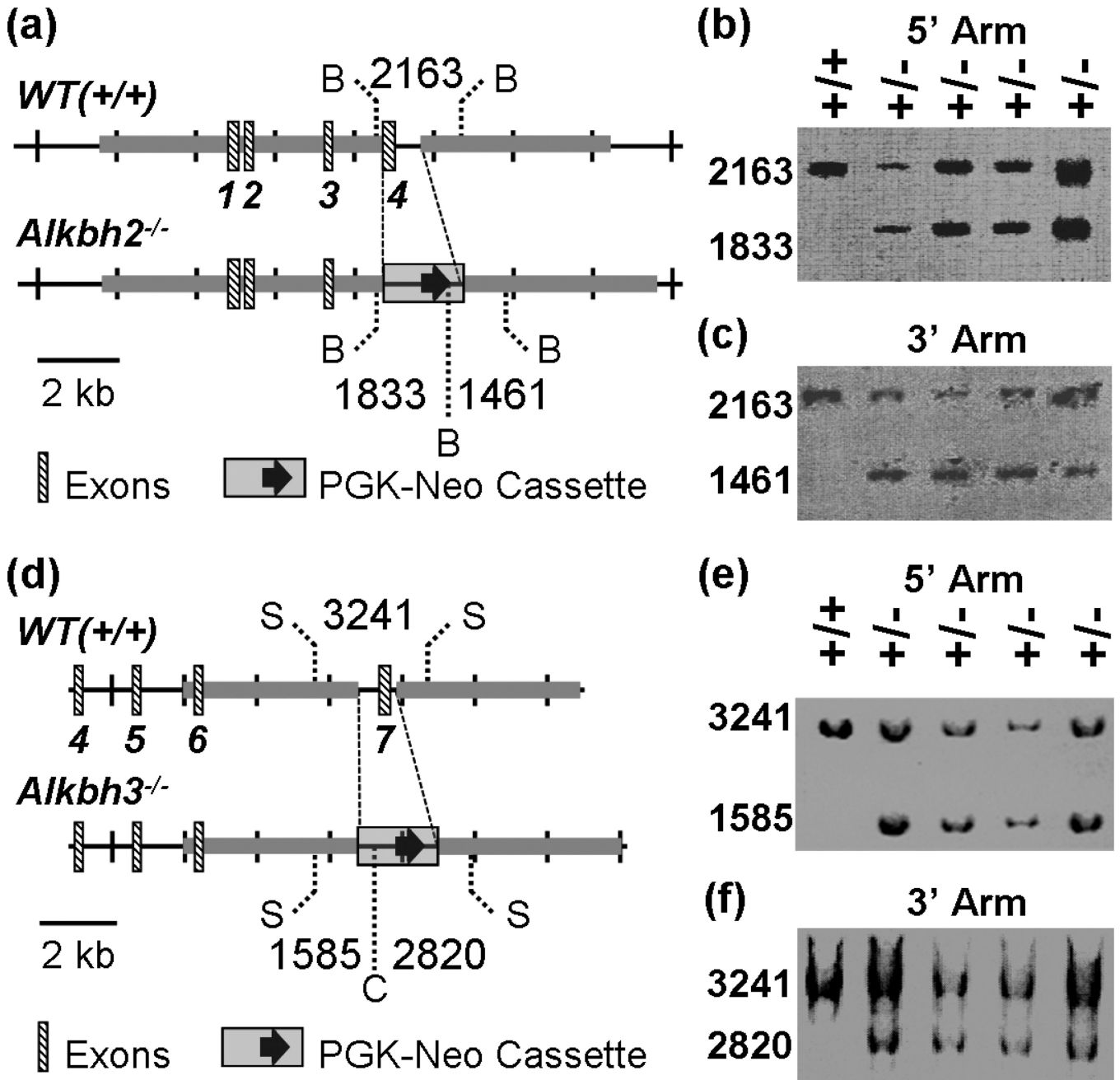


Figure 1. Maps for targeted deletions of mouse α -ketoglutarate/Fe(II) dioxygenases *Alkbh2* and *Alkbh3* were generated as follows: (a) *Alkbh2* and the site targeting the *Mus musculus* genomic sequence located on mouse chromosome 5 (LOCUS NC_000071 from the NCBI and Mouse Genome Sequencing Consortium). (b) Southern blots for *Alkbh2*^{+/-} heterozygotes using a probe for the 5' arm. +/+ is a WT control and +/- are different clones identified as heterozygotes by initial PCR screening. (c) Southern blots for *Alkbh2*^{+/-} heterozygotes using a probe for the 3' arm. +/+ is a WT control and +/- are different clones identified as heterozygotes by initial PCR screening. Clones used to probe (b) and (c) are identical. (d) *Alkbh3* and the site targeting the *Mus musculus* genomic sequence located on mouse chromosome 2 (LOCUS NC_000068 from the NCBI and Mouse Genome

Sequencing Consortium). (e) Southern blots for *Alkbh3*^{+/-} heterozygotes using a probe for the 5' arm. ++ is a WT control and +/- are for different clones identified as heterozygotes by initial PCR screening. (f) Southern blots for *Alkbh3*^{+/-} heterozygotes using a probe for the 3' arm. ++ is a WT control and +/- are for different clones identified as heterozygotes by initial PCR screening. Clones used to probe (e) and (f) are identical.

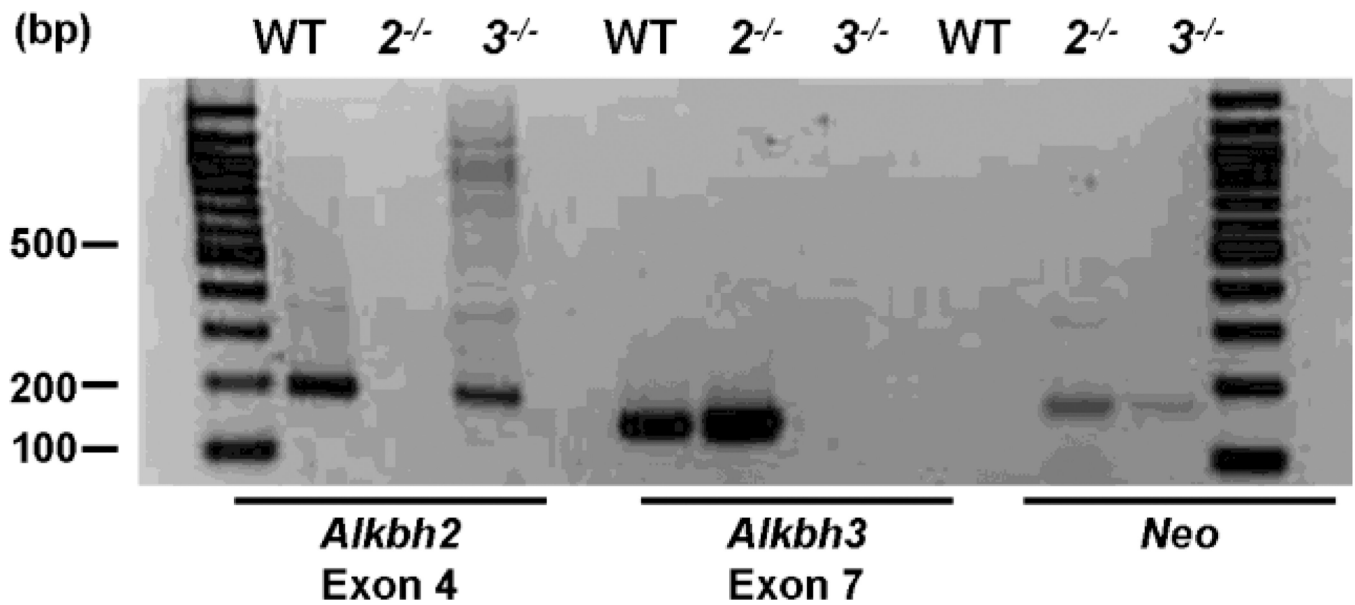


Figure 2. PCR confirmation of *Alkbh2* and *Alkbh3* targeted deletions was determined by amplification of deleted or inserted sequences in the *Alkbh2* or *Alkbh3* gene, using PCR. (a) The Exon 4 region of *Alkbh2*, the exon 7 region of *Alkbh3* and *Neo* gene contained in the cassette replacing *AlkBh2* or *AlkBh3* exons were amplified from genomic DNA extracted from primary WT and *Alkbh2* or *Alkbh3* knock-out MEFs. The 199 bp band is the product from Exon 4 of a functional *Alkbh2*. The 160 bp band is the product from Exon 7 of a functional *Alkbh3*. The 171 bp band is the neomycin PCR product found in the cassette used for targeted deletion of *Alkbh2* or *Alkbh3*.

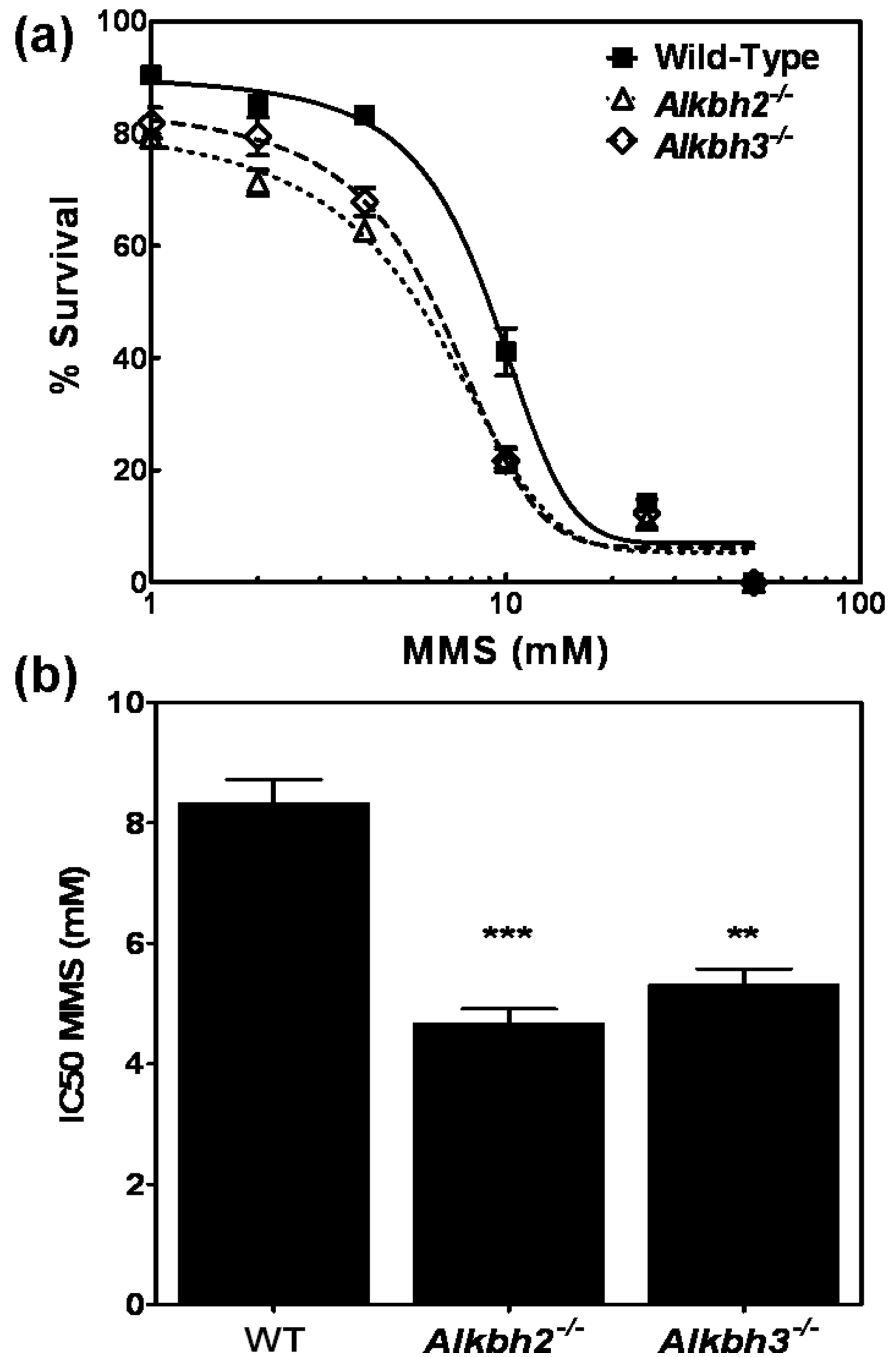


Figure 3. Cell survival of WT, *Alkbh2*^{-/-}, or *Alkbh3*^{-/-} primary Big Blue MEFs was determined 48 h post-treatment with MMS, as described in Experimental Procedures. (a) Survival was monitored using Trypan Blue staining to determine the percentage of intact cellular membranes in each culture. (b) IC₅₀ values for all the primary MEFs. All samples were analyzed in triplicate and with curve fitting and statistical analysis performed using Prism software. *** P equals 0.0003 and **P equals 0.003, compared to WT IC₅₀.

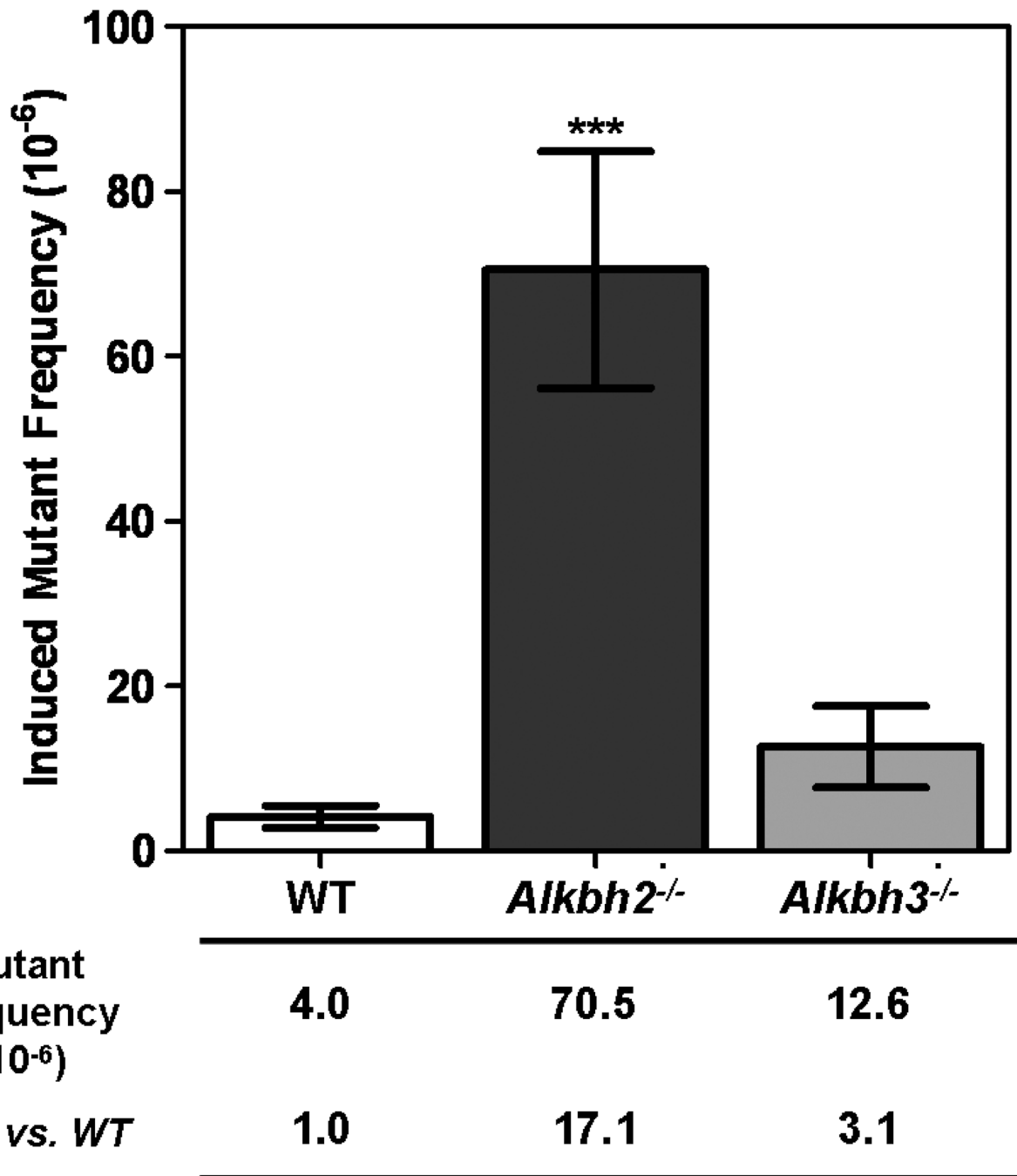


Figure 4. MMS-induced mutant frequencies for WT and *Alkbh2*^{-/-} or *Alkbh3*^{-/-} primary MEFs. Frequencies were determined by subtracting the spontaneous mutant frequency, as determined in G1250 cells infected with λ LIZ phage containing packaged *cII* genomic DNA, isolated from primary WT, *Alkbh2*, and *Alkbh3* knock-out MEFs, from the observed mutant frequency following 4 mM MMS treatment. *** P equals 0.0001.

WT (UN)/(MMS)

ACCACACCTATGGTGTATGCATTTATTTGCATACATTCAATCAATTGTTATCTAAGGAAA 60
 TACTTACATATGGTTTCGTGCAAACAAACGCAACGAGGCTCTACGAATCGAGAGTGCCTTG 120
 A T T T C C T
 AC A T TA A C CA C C A CT 180
 CTTAACAAAATCGCAATGCTTGGAAGTGAAGAAGACAGCGGAAGCTGTGGGCGTTGATAAG
 G TC T A T C C G A
 TCGCAGATCAGCAGGTGGAAGAGGGACTGGATTCCAAAGTTCTCAATGCTGCTTGCTGTT 240
 C G T C G G
 C C G T CT TC G
 CTTGAATGGGGGGTTCGTTGACGACGACATGGCTCGATTGGCGCGACAAGTTGCTGCGATT 300
 A C T
 CTCACCAATAAAAAACGCCCGGCGGCAACCGAGCGTTCTGAACAAATCCAGATGGAGTCC 360
 TGAGGTCATTACTGGATCTATCAACAGGAGTCATTATGACAAATACAGCAAAAATACTCA 420

Figure 5. Spontaneous and 4 mM MMS-induced mutation spectrum map from WT primary MEFs. 29 spontaneous and 36 MMS-induced mutants were sequenced. A 'v' indicates an insertion mutation. The exact number of each mutation type can be found in Table 2.

Alkbh2^{-/-} (UN)/(MMS)

ACCACACCTATGGTGTATGCATTTATTTGCATACATTCAATCAATTGTTATCTAAGGAAA 60
 TACTTACATATGGTTCGTGCAAACAAACGCAACGAGGCTCTACGAATCGAGAGTGCGTTG 120
 CTTAACAAAATCGCAATGCTTGGAACTGAGAAGACAGCGGAAGCTGTGGGCGTTGATAAG 180
 TCGCAGATCAGCAGGTGGAAGAGGGACTGGATTCCAAAGTTCTCAATGCTGCTTGCTGTT 240
 CTTGAATGGGGGGTCTTGAACGACGACATGGCTCGATTGGCGCGACAAGTTGCTGCGATT 300
 CTCACCAATAAAAAACGCCCGGCGCAACCGAGCGTTCTGAACAAATCCAGATGGAGTCC 360
 TGAGGTCATTAAGGATCTATCAACAGGAGTCATTATGACAAATACAGCAAAAATACTCA 420

Mutations indicated in red: AA, AA, AA, T, C, T, Tx2, C, A, C, T, C, C, C, A, A, AC, Tx17, TT, A, TA, C, T, G, A, A, TTA, A, T, TC, GT, TC, T, T, A, T, T, CTx2, G, Ax2, C, Ax4, TG, TG, 8x, A, C.

Figure 6. Spontaneous and 4 mM MMS-induced mutation spectrum map from *Alkbh2*^{-/-} primary MEFs. 54 spontaneous and 44 MMS-induced mutants were sequenced. A 'v' indicates an insertion mutation. The exact number of each mutation type can be found in Table 2.

Alkbh3^{-/-} (UN)/(MMS)

ACCACACCTATGGTGTATGCATTTATTTGCATACATTCAATCAATTGTTATCTAAGGAAA 60
 TACTTACATATGGTTCGTGCAAACAAACGCAACGAGGCTCTACGAATCGAGAGTGCGTTG 120
 CTTAACAAAATCGCAATGCTTGGAACTGAGAAGACAGCGGAAGCTGTGGGCGTTGATAAG 180
 TCGCAGATCAGCAGGTGGAAGAGGGACTGGATTCCAAAGTTCTCAATGCTGCTTGCTGTT 240
 CTTGAATGGGGGGT CGTTGACGACGACATGGCTCGATTGGCGCGACAAGTTGCTGCGATT 300
 CTCACCAATAAAAAACGCCCGCGGCAACCGAGCGTTCTGAACAAATCCAGATGGAGTCC 360
 TGAGGTCATTACTGGATCTATCAACAGGAGTCATTATGACAAATACAGCAAAAATACTCA 420

Mutations indicated in red: A, C, G, T, AC, T, A, A, A, T, T, C, A, GC, TGACA, G, TA, AC, A, Tx2, Ax2, Ax3, AA, T, TA, TT, G, A, A, TT, T, T, AT, TTT, T, A, A, C, T, AA, G, G, G, V, A, T, A, G, C, G, Tx4, A, Ax2, ACx2, T.

Figure 7. Spontaneous and 4 mM MMS-induced mutation spectrum map from *Alkbh3*^{-/-} primary MEFs. 43 spontaneous and 57 MMS-induced mutants were sequenced. A 'v' indicates an insertion mutation. The exact number of each mutation type can be found in Table 2.

Table 1

PCR primers. Primers listed were used for genotyping WT and *Alkbh2* or *Alkbh3* knock-out mouse colonies or genomic DNA extracted from WT and *Alkbh2*- or *Alkbh3*-deficient mouse embryonic fibroblasts.

Mouse Colony and Embryo Genotyping Primers			
cII-F	CCGCTCTTACACATTCCAGC	cII-R	CCTCTGCCGAAGTTGAGTAT
M2-F	GACCCTGCAGAGACCATT	E4-R	CTGCAAGCGCCAAAGGAGACA
M3-F	TTCTGGCACACACCACTAAGTCA	E7-R	ATCGTCGCTTGTGCCAGTCCA
		Neo-R	TGCTCAGCGGTGCTGCCATC
Mouse Embryonic Fibroblast PCR Primers			
E4-F	CACAGAGATGACGAGCGAGA	E4-R	TGTGGTACCAGTGGGTGTTG
E7-F	CCTGTGCTGTGGACTCTGAA	E7-R	AACTGAGGGAAGCAATGACG
Neo-F	CTGAATGAACTGCAGGACGA	Neo-R	ATACTTTCTCGGCAGGAGCA

Table 2

Spontaneous and MMS-induced mutation spectrum in WT and *Alkbh2* or *Alkbh3* knock-out MEFs. Mutation types are separated into eight categories. The number of mutants in each category is represented in bold and the percentage of the total number sequenced is in parentheses. Differences in spontaneous and MMS-induced mutation spectrum for WT and *Alkbh2* or *Alkbh3* knock-out MEFs is indicated as Fold Diff. The alternative mutation on the complementary DNA strand is also indicated. Mutations in columns vary significantly across rows ($p < 0.001$ by Monte Carlo-based chi square test).

Mutation Type	Wild Type			<i>Alkbh2</i> ^{-/-}			<i>Alkbh3</i> ^{-/-}		
	(-) MMS	(+) MMS	Fold Diff.	(-) MMS	(+) MMS	Fold Diff.	(-) MMS	(+) MMS	Fold Diff.
G→C C→G	6 (0.21)	3 (0.08)	0.4	5 (0.09)	3 (0.07)	0.7	3 (0.07)	2 (0.04)	0.5
G→T C→A	5 (0.18)	7 (0.19)	1.1	27 (0.50)	15 (0.34)	0.7	13 (0.30)	12 (0.21)	0.7
G→A C→T	3 (0.10)	8 (0.22)	2.2	11 (0.20)	14 (0.32)	1.6	15 (0.34)	16 (0.28)	0.8
T→A A→T	4 (0.14)	4 (0.11)	0.8	2 (0.04)	8 (0.18)	4.9	4 (0.09)	15 (0.26)	2.9
T→G A→C	6 (0.21)	3 (0.08)	0.4	3 (0.06)	3 (0.09)	1.2	3 (0.07)	4 (0.07)	1.0
T→C A→G	3 (0.10)	4 (0.11)	2.2	3 (0.06)	1 (0.023)	0.4	3 (0.07)	5 (0.09)	1.3
Insertion	2 (0.07)	6 (0.17)	2.4	3 (0.06)	0 (0.00)	0	0 (0.00)	2 (0.04)	2
Deletion	0 (0.00)	1 (0.03)	0	0 (0.00)	0 (0.00)	0	3 (0.07)	1 (0.02)	0.3
# Mutants Sequenced	29	36		54	44		43	57	